Light Transmission Through a Hollow Core Fiber Bundle

Md Abu Sufian , Erwan Baleine, Jeffrey Geldmeier, Ameen Alhalemi, Jose Enrique Antonio-Lopez,
Rodrigo Amezcua Correa, *Member, IEEE*, and Axel Schülzgen , *Fellow, IEEE*

Abstract—**This paper reports on the fabrication and performance of a fiber bundle with seven hollow cores arranged in a hexagonal pattern. The bundle shows individual core transmission with less than 0.07% core-to-core coupling over a length of 11 cm. Each core exhibits several transmission windows in the visible to near infrared region. These low attenuation regions with large higher order mode suppression are a result of anti-resonant guidance due to the negative curvature membranes encircling the cores. The central core exhibits the widest transmission window with a minimum loss of 4 dB/m between 1250 nm and 1450 nm. The lowest loss for the central core is estimated to be 2.5 dB/m at 600 nm. Such hollow core fiber bundles may be employed in applications including communication, imaging systems, high power laser delivery, or sensing.**

Index Terms—**Hollow core fiber, multicore fiber, fiber bundle, HCF bundle, HCF, PCF.**

I. INTRODUCTION

HOLLOW core fibers (HCFs) are a type of micro-structured fiber where light confinement is achieved in a core where the core solid material is removed. Compared to conventional fibers, HCFs offer a great potential of significant mitigation of material-imposed limitations such as transmission windows restricted by material absorption or optical power handling constrained by nonlinear optical effects or material damage. Over the last two decades, hollow core fiber technology has been explored as an alternative candidate to replace solid silica fibers [1], [2], [3]. In this effort, novel HCF fiber designs and fabrication techniques have been demonstrated to reduce the fiber loss and to extend their transmission windows. In contrast to conventional fibers, which carries light by total internal reflection (TIR), anti-resonant HCFs (AR HCFs) guide light exploiting the inhibited coupling, low overlap between core and capillary modes [4], and anti-resonance from the encircling glass

membranes [5] which provide improved light confinement. The membranes surrounding the core act as Fabry Perot resonators defining the high attenuation regions in the transmission spectrum while wavelengths away from these resonances exhibit better confinement due to small overlap between the core and glass modes. The resonant wavelength, λ_{res} can be obtained [6] from–

$$\lambda_{res} = \frac{4t\sqrt{n^2-1}}{2k+1}, \text{ where k = 1,2,3…} \qquad (1)$$

t is the capillary thickness, n is the refractive index of glass, and k is the order of the resonant wavelength.

Advanced AR HCFs have already surpassed silica fibers in terms of attenuation at fiber optic communication wavelengths in the O-band [7] and at mid-infrared wavelength (MIR) beyond $4\,\mu\text{m}$ [8], where silica absorption severely limits the transmission [9]. While solid core fiber technology is mature and considered to be the primary platform in optical communications and laser light delivery, novel AR HCF fiber designs still continue to improve in performance from UV to MIR wavelengths [10], [11], [12], [13]. In particular, the introduction of negative curvature designs [2], [14], [15], node-less lattice structures [16], and nested-capillary designs [17], [18] have enabled further improvement of AR HCF optical performances and the limits are still to be explored. The lack of solid core materials in HCFs allows low latency transmission [4], [19] since light travels at near vacuum speed in the hollow core and significantly enhances the power handling capabilities due to nonlinear optical effects [14]. In the last few years, transmission of high peak power ns/ps pulses [20], fs pulses [21], [22], and kW average power [23], [24] through AR HCFs have been reported. Owing to the progress in HCF technology, they are considered to be a potential rival to replace solid core silica fibers in many applications and are opening new avenues for fiber optics [10], [11], [17], [18], [25].

Amongst the promising application areas of HCFs are medical imaging and diagnostics. Imaging fibers are typically bundles, where many individual fibers or fibers cores are densely packed together to form a multi-core structure [26]. In addition to medical imaging [27], [28], [29], multicore fibers and bundles have been employed in numerous applications including optical fiber communication [30], [31], [32], sensing [33], [34], [35], [36], [37], fiber lasers [38], [39], [40], fiber couplers [41], to name but a few.

One major limiting factor of fiber bundles, particularly for imaging applications, is core-to-core crosstalk. A conspicuous

approach to limit the crosstalk between adjacent cores is to increase the core separation and the mode confinement [42]. However, these weakly coupled fibers impose restrictions on the fiber design and the operating wavelength range. In addition, the imaging resolution is reduced while the fiber diameter increases. An alternative solution is to employ disordered lattice structure, where anti-symmetry reduces the modal overlap between neighboring cores resulting in reduced coupling efficiency which enables decoupled modes propagating through individual cores [43]. On the other hand, multi-core structures with small core-to-core distances exhibit strong coupling between cores and the formation of supermodes [44]. Such supermodes can be considered the eigenmodes that extend over the waveguide cross-section and remain invariant along the fiber length [45]. In general, the optical fields propagating inside a multi-core structure can be described using the coupled-mode equation given by [46]–

$$\frac{dA_m(z)}{dz} = -j \sum_{n \neq m} \kappa_{nm} \times A_n(z) \times e^{j\Delta\beta_{mn}z} \times \phi(z) \quad (2)$$

where A_m and A_n are mode field amplitude distributions in cores m and n respectively, $\phi(z)$ is a random phase function which takes into account bending and twisting effects of the fiber, and $\Delta\beta_{mn} = \beta_m - \beta_n$, where β_m and β_n are propagation constants of the modes in cores m and n respectively.

According to the coupled mode theory, the mode coupling coefficient κ_{nm} from core n to m is determined by the overlap integral of the corresponding guided modes for each individual core, [47], [48]–

$$\kappa_{nm} = \frac{k_0^2}{2\beta_m} \frac{\iint \Delta\epsilon_{rm} A_m A_n dS_\infty}{\iint A_n^2 dS_\infty} \quad (3)$$

where k_0 is the wave number in free space, S_∞ is the infinite cross-sectional area and $\Delta\epsilon_{rm} = n_{core,m}^2 - n_{clad}^2$. While the coupled-mode theory can describe the statistical nature of the coupling strength between two cores, a more accurate approach to obtain the coupling coefficient is the supermode theory. Here, the eigenvalue problem of the waveguide is solved, and the propagation constants can then be used to estimate the coupling efficiency.

In this paper, our research focuses on the analysis of the light propagation in a fiber bundle formed by hollow cores distributed in a hexagonal pattern. The choice of a hexagonal distribution is warranted since it offers the maximum core density, for 7 cores, 19 cores, 37 cores, etc. [45], [49], [50]. Here, we propose and demonstrate a 7-core hollow core fiber bundle (HCFB) where each core forms an anti-resonant waveguide exploiting the inhibited coupling in a negative curvature design. The bundle is drawn in house using the popular stack and draw method. The hexagonal 6 capillary cladding architecture allows for a dense multicore design with a small distance between neighboring cores. On one hand, such small core-to-core pitch might introduce some core-to-core coupling that could impede high-quality imaging due to the superposition of modes [51]. On the other hand, nonuniformities introduced during the fabrication process reduce the mode overlap and potentially reduces the coupling
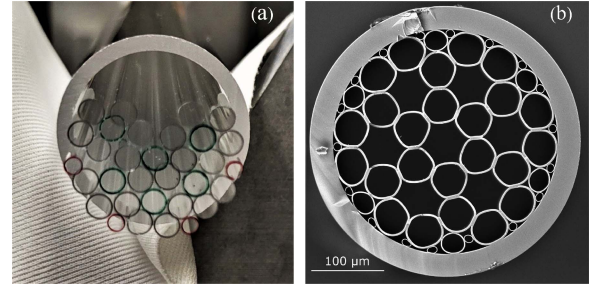

Fig. 1. Fabrication of the hollow core fiber bundle by the stack and draw method. (a) A stack (ϕ 25 mm) of the bundle structure with a suitable arrangement of glass capillaries, (b) SEM image of the fiber bundle cross section (ϕ 375 μm) drawn from the preform. The light grey regions are the cladding glass microstructures, whereas the black regions represent fiber bundle areas filled by air.

efficiency significantly [52]. Unlike multicore fibers, where core-to-core coupling may be desired for supermode formation, minimization of crosstalk is among the desired features of fiber bundles. In this paper, we analyze the core-to-core coupling in our HCFB experimentally and through simulations using the finite element mode solver provided by COMSOL. Experiments and simulations demonstrate that even small non-uniformities prohibit the formation of supermodes and strongly decouple the transmission of individual hollow core.

II. FABRICATION AND CHARACTERIZATION

The HCFB, shown in Fig. 1(b), consists of seven hollow cores, each surrounded by six glass capillaries forming claddings with negative curvatures. The fiber bundle is fabricated using a two-stage stack-and-draw method. In the first stage, shown in Fig. 1(a), fused silica capillaries are stacked inside a larger jacket tube. The HCFB is drawn to its final dimensions with an outer diameter of 375 μm. The cross-section of the drawn fiber bundle is shown in Fig. 1(b). The SEM image reveals the HCFB geometry with a central core diameter of 54.2 μm, capillary diameters of about 44 μm, and capillary thicknesses of about 2.9 μm. While the overall structure of all seven hollow cores are similar, slight differences between individual cores due to the fabrication process are also indicated in Fig. 1(b).

Transmission spectra of individual cores are obtained using a broadband light source (SuperK Compact by NKT Photonics) and an optical spectrum analyzer (AQ6370B by Yokogawa). Each core is excited by imaging the facet of the supercontinuum laser delivery fiber (SMF28) onto individual cores of the HCFB using a pair of aspheric lenses. At the output facet of the 1.7 m fiber, two circular irises are employed to spatially filter out the transmission modes of the individual capillaries. This procedure is repeated several times for each fiber core. While both ends of the fiber are clamped on to nano-stages, the mid-section of the fiber is spooled in a single loop with a diameter exceeding 50 cm. A large bend radius helps to keeps the bending loss to a minimum [8].

Normalized transmission spectra for cores 1, 2 and 3 are shown in Fig. 2(a). For better visibility we only show transmission spectra for 3 cores while the other 4 cores exhibit very
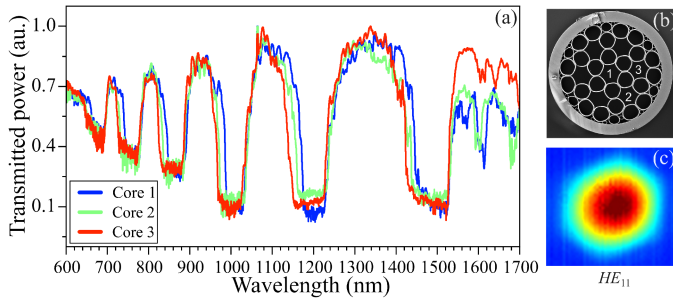
Fig. 2. (a) Normalized transmission spectrum of cores 1, 2 and 3, as denoted in (b) SEM of fiber bundle. (c) The transmitted fundamental mode (HE_{11}) for the central core at a wavelength of 1550 nm.
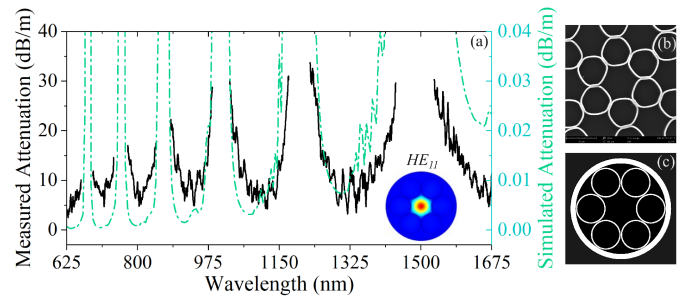

Fig. 3. (a) Measured vs. simulated attenuation spectrum of the fiber bundle. The measurements of attenuation within the central core of the bundle shown in (b) are performed using the cut-back method. Multiple high and low attenuation regions can be observed and reproduced in simulations considering the fundamental air-core mode in the idealized structure shown in (c).

similar transmission. Each spectrum exhibits multiple windows of high transmittance and high attenuation. Here the high attenuation bands correspond to 4th to 9th order resonances, going from longer to shorter wavelengths, see 1. Spectral locations of these high attenuation regions are determined by the membrane thickness. The measurement range of the spectra is limited by the OSA (600 nm to 1700 nm).

Although the dominant features are similar for all cores, some variations can also be observed because individual cores differ slightly in core diameter, curvature of the surrounding membranes, capillary shapes, and node sizes. For instance, core 1 has the largest diameter of 54.2 μm, followed by core 2 and core 3. The average diameter of core 2 and core 3 are 51.2 μm and 49.5 μm, respectively. For this bundle it is found that the high attenuation band edges for core 3 are located at shorter wavelengths compared to cores 2 and 1 resulting in slightly smaller windows of high transmission. In addition, the capillary junctions or nodes, where adjacent tubes touch and fuse together, have different thicknesses than the glass membranes. These nodes surrounding the cores introduce additional losses within the transmission windows [53]. This is particularly evident near 1600 nm where the node resonance causes a dip in the transmission spectrum for all the three cores.

III. SIMULATIONS

The commercial finite element mode solver COMSOL is used to simulate the transmission spectrum that corresponds to the central core structure of the bundle cross section shown in Fig. 3(b). As shown in Fig. 3(c), the 2D COMSOL model features an idealized transverse structure where the capillaries are perfectly circular and symmetric. This disparity between simulations and experiments was chosen to significantly reduce the necessary computation resources that would be required considering the actual geometry. As seen in Fig. 3(a), our COMSOL simulations cover the whole wavelength range of the experimental data using reasonable computation times of a few hours. The simulated attenuation spectrum exclusively accounts for confinement losses, leakage and bending losses are not taken into consideration in this work.

Fig. 3(a) compares the attenuation spectra obtained from both experimental measurements and model simulations. The

experimental attenuation spectrum shown is obtained using the cutback method with the broadband light source launched into the central core. We started with an initial length of the fiber bundle of 1.71 m and cut back to a length of 21 cm. While the simulated geometry deviates from the actual fiber, the main anti-resonant transmission features of spectra are in good agreement. The low-attenuation windows are positioned at similar wavelengths and their bandwidths widen from short to longer wavelengths. Experimentally, the lowest confinement loss of 2.5 dB/m is measured at 600 nm. The widest transmission band is found between 1250nm-1450 nm, with minimum losses around 4 dB/m.

Unsurprisingly, the simulated loss is 3 orders of magnitude lower than that of the experimental results. This is due to the imperfect transverse bundle structure and possible, but unknown, local non-uniformity along the propagation direction which contribute to the increase in attenuation. While the perfect circular structures and the node-less fiber geometry of the model results in very good mode confinement and low losses in the simulations, the presence of capillary nodes surrounding the core in the real fiber bundle introduces additional resonance within the transmission windows [53], further downgrading the experimental loss profile of the fiber bundle.

IV. CORE-TO-CORE COUPLING

When two or more waveguides are in proximity, one can apply coupled-mode theory that assumes the presence of additional waveguides to be a small perturbation to the original single waveguide problem. On the other hand, if a fiber consists of multiple cores, i.e., in a multicore fiber bundle, the eigenmodes of the structure can be obtained by solving wave equations across the whole fiber geometry, including all coupled cores. These multi-waveguide eigenmodes are usually called supermodes. Simultaneous propagation of these supermodes leads to a changing field distribution across the multiple cores in the propagation direction [54]. In our fiber bundle the cores are closely packed and are separated by a layer of capillaries. Similar to a multi-core fiber, there may be crosstalk between neighboring cores, hence supermodes. To investigate how supermodes form
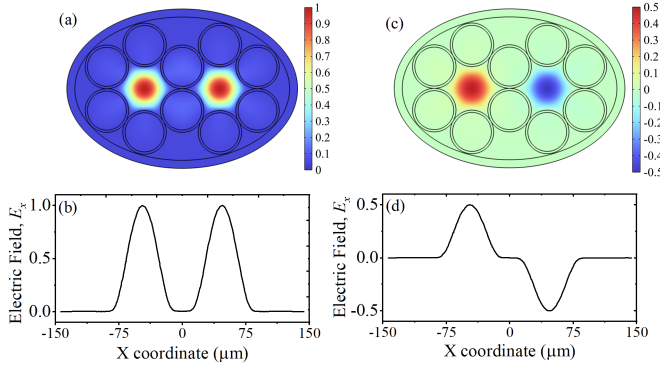
Fig. 4.   Supermodes of a twin-hollow-core fiber. (a) 2D and (b) 1D electric field distributions of the even (in-phase) mode where the fields have the same phases in both cores, (c) 2D and (d) 1D electric field distributions of the odd (out-of-phase) mode where fields in both cores have opposite phases.

in a multi-core structure, twin-core and seven-core hollow core structures have been studied [52].

A. The Idealized Twin-Hollow-Core Fiber Structure

It has been shown that twin-core fibers can sufficiently represent and provide insight into the modal characteristics of a multicore structure [52]. According to supermode theory, the eigenmodes of such system are first-order and second-order supermodes, and their eigen values, i.e., propagation constants, are β_{even} and β_{odd} [55]. E_{even} and E_{odd} describe the supermode electric field distributions. Here, we consider a system of two coupled single mode waveguides. The whole structure features two orthogonally polarized eigenstates (supermodes) and the sum of these mode fields is the total electric field propagating along the fiber. Hence, the total power intensity is defined as–

$$I = |E_{even} + E_{odd}|^2$$
$$= |E_{even}|^2 + |E_{odd}|^2 + 2E_{even}E_{odd}\cos(\Delta\beta z) \quad (4)$$

where $\Delta\beta = \beta_{even} - \beta_{odd}$, defines the beating term. Estimated $\Delta\beta$ can be used to obtain the beat length, $L_c = \frac{\pi}{\Delta\beta} = \pi \times [k_0(n_{eff}^{even} - n_{eff}^{odd})]^{-1}$, [56], [57] which is described as the smallest length over which the power of one core is completely transferred to the other. The beat length derived here based on the supermode theory can be readily used to estimate $\kappa' = \frac{\Delta\beta}{2}$ [58], the supermode coupling coefficient. Here, κ' quantifies the power coupling from the initially excited supermode to the initially un-excited supermode. This is similar to the coupling of guided modes of different cores in coupled mode theory when the coupling of separate waveguides is quantified by κ_{nm}, as defined in (3).

Fig. 4 shows the even and odd modes of the idealized twin-hollow-core fiber where both cores have a geometry similar to the hollow core used for the above discussed simulations, see Fig. 3(c). The highest index mode here represents the even mode where the field amplitudes are symmetric and equally distributed between the two cores. The second order supermode (odd mode) has an antisymmetric electric field distribution with field phase reversal between the cores. The total power of each supermode
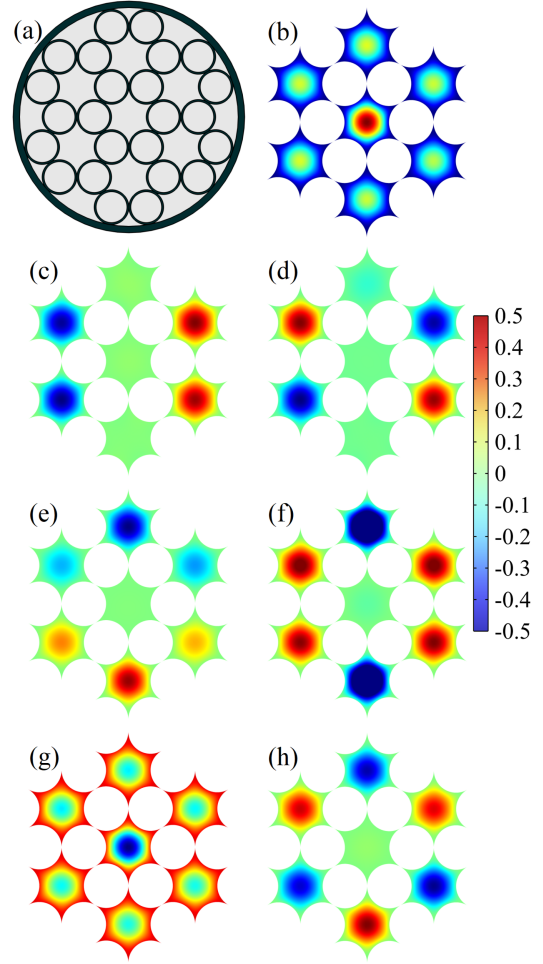

Fig. 5.   (a) Idealized 7-hollow-core fiber bundle cross section. (b)–(h) Computed 2D electric field distributions for the 7 supermodes supported by the bundle structure.

is distributed evenly between the cores for both modes. It is to be noted that each index mode also allows polarization dependent degeneracy. The effective refractive indices n_{eff}^{even} and n_{eff}^{odd} are obtained from the eigenvalues β^{even} and β^{odd} provided by the COMSOL simulation, respectively. The coupling is very weak, and the coupling coefficient is calculated to be $8.02 \times 10^{-7}\mu m^{-1}$ which corresponds to a beat length of 1.94 m at 1550 nm.

B. Fiber Bundle With Seven Hollow Cores

In order to identify the supermodes in a HCFB with seven hollow cores, the geometry of a symmetric idealized HCFB structure (Fig. 5(a)) is simulated with COMSOL. Solving the boundary value problem across the whole cross-section for a wavelength of 1550 nm, 7 distinctive modes can be identified. The corresponding electric field distributions are presented in Fig. 5(b)– (h). The fundamental supermode (Fig. 5(b)), with the largest effective index, exhibits a LP_{01}-like or degenerate HE_{11} mode structure. The second (Fig. 5(c)) and third (Fig. 5(d)) supermodes have a symmetric and anti-symmetric LP_{11}-like mode structure (superposition of degenerate TE_{01},
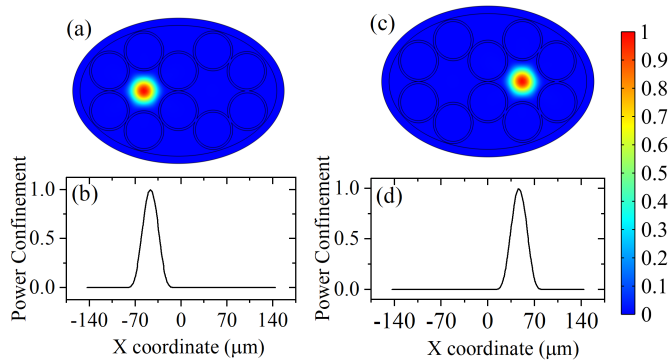
Fig. 6.   Asymmetric twin-core fiber model. 2D and 1D power distributions in the (a)–(b) left core, and (c)–(d) right core. No supermode field distributions are found.

TM_{01}, HE_{21} modes). The fourth (Fig. 5(e)) and fifth (Fig. 5(f)) supermodes are LP_{21}-like modes (superposition of degenerate EH_{11}, HE_{31} modes). The sixth supermode (Fig. 5(g)) exhibits LP_{02}-like geometry (degenerate HE_{12} mode), while the seventh supermode (Fig. 5(h)) shows LP_{31} mode (superposition of HE_{41} and EH_{21} degenerate modes). Each supermode is two-fold polarization degenerate.

C. Non-Uniform Twin-Hollow-Core Fiber Structure

Although the simulation results show the support of 7 supermodes (14 considering the polarization degeneracy) in the 7-core structure, no supermode field distribution is observed in our fiber bundle experiments. Our simulations indicate that this can be attributed to the fabrication induced transverse nonuniformity across the fiber cross-section. Non-uniformity and asymmetric geometry truncate the field overlap between adjacent cores, hence, reduce the coupling efficiency. A twin-core slightly distorted structure is modeled to support this assumption. As for the idealized structure considered previously, the coupling coefficient, beat length, and coupling efficiency are calculated. Compared to the idealized structure in Fig. 4, the diameters of the two right-most capillaries in Fig. 6 are reduced by only 1%. Albeit small, the induced dissimilarity between left and right core is sufficient to eliminate the support of supermodes. Rather, the mode profiles resemble that of two decoupled independent fibers with single hollow cores. At 1550 nm, the beat length in the distorted structure is reduced to 0.142 m, a 92.7% reduction from the symmetric model. The coupling coefficient, estimated to be 1.1×10^{-5} μm^{-1}, increased by one order of magnitude, similar to the findings in [59]. Despite the increase in coupling coefficient, the coupling efficiency in the antisymmetric structure is greatly reduced and power transfer between the cores is practically negligible. The coupling efficiency, which quantifies the fraction of power transferred from one core to the other following propagation over the beat length, drops from 100% (in a symmetric structure) to 0.13% in the asymmetric fiber model. In Fig. 6(c)–(d), 99.87% of the total power is confined in one core. This effect is more evident in large core fibers where fabrication induced imperfections drastically reduce the coupling efficiency,

causing the eigenmodes to reduce to independent core modes [52].

D. Experimental Core-to-Core Coupling in the HCFB

An experimental setup is arranged to determine the coupling between adjacent cores in the HCFB. Only the central core is excited. After propagation through several lengths of the bundle, spanning from 11 cm to 1.71 m, the transmitted powers exiting from the other cores are recorded to quantify core-to-core coupling experimentally. Within the measurement limits of 0.07%, no power transfer between the central and outer cores is observed. It can be inferred that the structural imperfections and reduced symmetry of the actual bundle structure introduced during the fiber draw process reduces the core-to-core coupling in the HCFB to an insignificant value for the lengths examined. This negligible coupling between cores in the multicore bundle indicates that the formation of supermodes is prohibited in our HCFB, unlike prior reports on supermode based sensors [33] and laser system [60] with solid core multicore fibers.

V. CONCLUSION

In conclusion, we demonstrated, for the first time in our knowledge, light transmission through a multi-core hollow core fiber bundle. Due to the imperfect symmetry of our 7 HCFB, supermode formation is suppressed and independent individual core modes are supported. Each core exhibits multiple transmission windows with the transmission windows defined by their corresponding core architecture. The lowest attenuation is observed around 600 nm for the central core. Although the measured loss in this fiber bundle is significantly larger than in antiresonant silica fibers with a single hollow core, similar HCFBs may find important application in imaging and short-range data transmission. Additionally, further performance improvement via curvature enhancement and node-reduction can be realized providing further avenues for practical uses. Since hollow core fiber high attenuation regions can be tuned by controlling the capillary thicknesses, the transmission windows can be shifted to a pertaining wavelength for different applications. Scaled up fiber bundles with increased number of cores have potential for high resolution imaging and space division multiplexing in optical communications.

REFERENCES

[1] R. F. Cregan et al., "Single-mode photonic band gap guidance of light in air," *Science*, vol. 285, no. 5433, pp. 1537–1539, Sep. 1999, doi: 10.1126/science.285.5433.1537.

[2] Y. Y. Wang, N. V. Wheeler, F. Couny, P. J. Roberts, and F. Benabid, "Low loss broadband transmission in hypocycloid-core Kagome hollow-core photonic crystal fiber," *Opt. Lett.*, vol. 36, no. 5, pp. 669–671, Mar. 2011. [Online]. Available: https://opg.optica.org/abstract.cfm?URI=ol-36-5-669

[3] F. Yu and J. C. Knight, "Negative curvature hollow-core optical fiber," *IEEE J. Sel. Topics Quantum Electron.*, vol. 22, no. 2, pp. 146–155, Mar.-Apr. 2016. [Online]. Available: https://ieeexplore.ieee.org/document/7225120/

[4] F. Couny, F. Benabid, P. J. Roberts, P. S. Light, and M. G. Raymer, "Generation and photonic guidance of multi-octave optical-frequency combs," *Science*, vol. 318, no. 5853, pp. 1118–1121, Nov. 2007. [Online]. Available: https://www.science.org/doi/10.1126/science.1149091

[5] M. A. Duguay, Y. Kokubun, T. L. Koch, and L. Pfeiffer, "Antiresonant reflecting optical waveguides in SiO_2-Si multilayer structures," *Appl. Phys. Lett.*, vol. 49, no. 1, pp. 13–15, Jul. 1986. [Online]. Available: http://aip.scitation.org/doi/10.1063/1.97085

[6] N. M. Litchinitser, A. K. Abeeluck, C. Headley, and B. J. Eggleton, "Antiresonant reflecting photonic crystal optical waveguides," *Opt. Lett.*, vol. 27, no. 18, pp. 1592–1594, Sep. 2002. [Online]. Available: https://opg.optica.org/abstract.cfm?URI=ol-27-18-1592

[7] G. T. Jasion et al., "0.174 dB/km hollow core double nested antiresonant nodeless fiber (DNANF)," in *Proc. Opt. Fiber Commun. Conf.*, 2022, Paper Th4C.7. [Online]. Available: https://opg.optica.org/abstract.cfm?URI=OFC-2022-Th4C.7

[8] A. V. Newkirk, J. E. Antonio-Lopez, R. A. Correa, and A. Schülzgen, "Extending the transmission of a silica hollow core fiber to 4.6 μm," *Opt. Continuum*, vol. 1, no. 9, Sep. 2022, Art. no. 2062. [Online]. Available: https://opg.optica.org/abstract.cfm?URI=optcon-1-9-2062

[9] R. Kitamura, L. Pilon, and M. Jonasz, "Optical constants of silica glass from extreme ultraviolet to far infrared at near room temperature," *Appl. Opt.*, vol. 46, no. 33, Nov. 2007, Art. no. 8118. [Online]. Available: https://opg.optica.org/abstract.cfm?URI=ao-46-33-8118

[10] T. D. Bradley et al., "Record low-loss 1.3 dB/km data transmitting antiresonant hollow core fibre," in *Proc. IEEE Eur. Conf. Opt. Commun.*, 2018, pp. 1–3. [Online]. Available: https://ieeexplore.ieee.org/document/8535324/

[11] T. Bradley et al., "Antiresonant hollow core fibre with 0.65 dB/km attenuation across the C and L telecommunication bands," in *Proc. 45th Eur. Conf. Opt. Commun.*, 2019, pp. 1–4. [Online]. Available: https://digital-library.theiet.org/content/conferences/10.1049/cp.2019.1028

[12] G. T. Jasion et al., "Hollow core NANF with 0.28 dB/km attenuation in the C and L bands," in *Proc. Opt. Fiber Commun. Conf. Postdeadline Papers*, 2020, Paper Th4B.4. [Online]. Available: https://opg.optica.org/abstract.cfm?URI=OFC-2020-Th4B.4

[13] H. Sakr et al., "Hollow core optical fibres with comparable attenuation to silica fibres between 600 and 1100 nm," *Nature Commun.*, vol. 11, no. 1, Dec. 2020, Art. no. 6030. [Online]. Available: http://www.nature.com/articles/s41467-020-19910-7

[14] N. V. Wheeler et al., "Low-loss Kagome hollow-core fibers operating from the near- to the mid-IR," *Opt. Lett.*, vol. 42, no. 13, Jul. 2017, Art. no. 2571. [Online]. Available: https://opg.optica.org/abstract.cfm?URI=ol-42-13-2571

[15] A. F. Kosolapov et al., "Hollow-core revolver fibre with a double-capillary reflective cladding," *Quantum Electron.*, vol. 46, no. 3, pp. 267–270, Mar. 2016. [Online]. Available: http://stacks.iop.org/1063-7818/46/i=3/a=267?key=crossref.c79969f84cfe828474fee924e41a397f

[16] A. N. Kolyadin et al., "Light transmission in negative curvature hollow core fiber in extremely high material loss region," *Opt. Exp.*, vol. 21, no. 8, Apr. 2013, Art. no. 9514. [Online]. Available: https://opg.optica.org/oe/abstract.cfm?uri=oe-21-8-9514

[17] W. Belardi and J. C. Knight, "Hollow antiresonant fibers with reduced attenuation," *Opt. Lett.*, vol. 39, no. 7, Apr. 2014, Art. no. 1853. [Online]. Available: https://opg.optica.org/abstract.cfm?URI=ol-39-7-1853

[18] F. Poletti, "Nested antiresonant nodeless hollow core fiber," *Opt. Exp.*, vol. 22, no. 20, Oct. 2014, Art. no. 23807. [Online]. Available: https://opg.optica.org/oe/abstract.cfm?uri=oe-22-20-23807

[19] F. Poletti et al., "Towards high-capacity fibre-optic communications at the speed of light in vacuum," *Nature Photon.*, vol. 7, no. 4, pp. 279–284, Apr. 2013. [Online]. Available: http://www.nature.com/articles/nphoton.2013.45

[20] P. Jaworski et al., "Picosecond and nanosecond pulse delivery through a hollow-core negative curvature fiber for micro-machining applications," *Opt. Exp.*, vol. 21, no. 19, Sep. 2013, Art. no. 22742. [Online]. Available: https://opg.optica.org/oe/abstract.cfm?uri=oe-21-19-22742

[21] B. Debord et al., "Multi-meter fiber-delivery and pulse self-compression of milli-joule femtosecond laser and fiber-aided laser-micromachining," *Opt. Exp.*, vol. 22, no. 9, Art. no. 10735, May 2014. [Online]. Available: https://opg.optica.org/abstract.cfm?URI=oe-22-9-10735

[22] S. Eilzer and B. Wedel, "Hollow core optical fibers for industrial ultra short pulse laser beam delivery applications," *Fibers*, vol. 6, no. 4, Art. no. 80, Oct. 2018. [Online]. Available: http://www.mdpi.com/2079-6439/6/4/80

[23] G. Palma-Vega et al., "High average power transmission through hollow-core fibers," in *Proc. Adv. Solid State Lasers Congr.*, 2018, Paper ATh1A.7. [Online]. Available: https://opg.optica.org/abstract.cfm?URI=ASSL-2018-ATh1A.7

[24] M. A. Cooper et al., "KW single mode CW laser transmission in an anti-resonant hollow-core fiber," in *Proc. Laser Technol. Defense Secur.*, 2022, Art. no. 19. [Online]. Available: https://www.spiedigitallibrary.org/conference-proceedings-of-spie/PC12092/2619034/KW-single-mode-CW-laser-transmission-in-an-anti-resonant/10.1117/12.2619034.full

[25] S.-F. Gao et al., "Hollow-core conjoined-tube negative-curvature fibre with ultralow loss," *Nature Commun.*, vol. 9, no. 1, Dec. 2018, Art. no. 2828. [Online]. Available: http://www.nature.com/articles/s41467-018-05225-1

[26] B. A. Flusberg et al., "Fiber-optic fluorescence imaging," *Nature Methods*, vol. 2, no. 12, pp. 941–950, Dec. 2005. [Online]. Available: http://www.nature.com/articles/nmeth820

[27] A. F. Gmitro and D. Aziz, "Confocal microscopy through a fiber-optic imaging bundle," *Opt. Lett.*, vol. 18, no. 8, Apr. 1993, Art. no. 565. [Online]. Available: https://opg.optica.org/abstract.cfm?URI=ol-18-8-565

[28] W. Göbel, J. N. D. Kerr, A. Nimmerjahn, and F. Helmchen, "Miniaturized two-photon microscope based on a flexible coherent fiber bundle and a gradient-index lens objective," *Opt. Lett.*, vol. 29, no. 21, Nov. 2004, Art. no. 2521. [Online]. Available: https://opg.optica.org/abstract.cfm?URI=ol-29-21-2521

[29] K. L. Reichenbach and C. Xu, "Numerical analysis of light propagation in image fibers or coherent fiber bundles," *Opt. Exp.*, vol. 15, no. 5, 2007, Art. no. 2151. [Online]. Available: https://opg.optica.org/oe/abstract.cfm?uri=oe-15-5-2151

[30] R.-J. Essiambre, R. Ryf, N. K. Fontaine, and S. Randel, "Breakthroughs in photonics 2012: Space-division multiplexing in multimode and multicore fibers for high-capacity optical communication," *IEEE Photon. J.*, vol. 5, no. 2, Apr. 2013, Art no. 0701307. [Online]. Available: https://ieeexplore.ieee.org/document/6508867/

[31] R. G. H. v. Uden et al., "Ultra-high-density spatial division multiplexing with a few-mode multicore fibre," *Nature Photon.*, vol. 8, no. 11, pp. 865–870, Nov. 2014. [Online]. Available: http://www.nature.com/articles/nphoton.2014.243

[32] Y. Kokubun and M. Koshiba, "Novel multi-core fibers for mode division multiplexing: Proposal and design principle," *IEICE Electron. Exp.*, vol. 6, no. 8, pp. 522–528, 2009. [Online]. Available: http://www.jstage.jst.go.jp/article/elex/6/8/6_8_522/_article

[33] A. V. Newkirk, E. Antonio-Lopez, G. Salceda-Delgado, R. Amezcua-Correa, and A. Schülzgen, "Optimization of multicore fiber for high-temperature sensing," *Opt. Lett.*, vol. 39, no. 16, Aug. 2014, Art. no. 4812. [Online]. Available: https://opg.optica.org/abstract.cfm?URI=ol-39-16-4812

[34] J. E. Antonio-Lopez, Z. S. Eznaveh, P. LiKamWa, A. Schülzgen, and R. Amezcua-Correa, "Multicore fiber sensor for high-temperature applications up to 1000°C," *Opt. Lett.*, vol. 39, no. 15, Aug. 2014, Art. no. 4309. [Online]. Available: https://opg.optica.org/abstract.cfm?URI=ol-39-15-4309

[35] J. Villatoro et al., "Composed multicore fiber structure for direction-sensitive curvature monitoring," *APL Photon.*, vol. 5, no. 7, Jul. 2020, Art. no. 070801, doi: 10.1063/1.5128285.

[36] L. Yuan and X. Wang, "Four-beam single fiber optic interferometer and its sensing characteristics," *Sensors Actuators A: Phys.*, vol. 138, no. 1, pp. 9–15, Jul. 2007. [Online]. Available: https://linkinghub.elsevier.com/retrieve/pii/S0924424707003135

[37] G. Salceda-Delgado, A. Van-Newkirk, J. E. A. Lopez, A. Schülzgen, and R. A. Correa, "Optical fiber curvature sensors based on single mode - 7 core - single mode fiber structures," in *Proc. Adv. Photon.*, 2014, Paper SeW3C.2. [Online]. Available: https://opg.optica.org/abstract.cfm?URI=Sensors-2014-SeW3C.2

[38] Y. Huo and P. K. Cheo, "Analysis of transverse mode competition and selection in multicore fiber lasers," *J. Opt. Soc. Amer. B*, vol. 22, no. 11, Nov. 2005, Art. no. 2345. [Online]. Available: https://opg.optica.org/abstract.cfm?URI=josab-22-11-2345

[39] C. Jollivet et al., "Mode-resolved gain analysis and lasing in multi-supermode multi-core fiber laser," *Opt. Exp.*, vol. 22, no. 24, Dec. 2014, Art. no. 30377. [Online]. Available: https://opg.optica.org/oe/abstract.cfm?uri=oe-22-24-30377

[40] A. Klenke, C. Jauregui, A. Steinkopff, C. Aleshire, and J. Limpert, "High-power multicore fiber laser systems," *Prog. Quantum Electron.*, vol. 84, Jun. 2022, Art. no. 100412. [Online]. Available: https://linkinghub.elsevier.com/retrieve/pii/S0079672722000386

[41] H. Zhang et al., "A tuneable multi-core to single mode fiber coupler," *IEEE Photon. Technol. Lett.*, vol. 29, no. 7, pp. 591–594, Apr. 2017. [Online]. Available: https://ieeexplore.ieee.org/document/7864376/

[42] Z. Zhao, Y. Dang, and M. Tang, "Advances in multicore fiber grating sensors," *Photonics*, vol. 9, no. 6, May 2022, Art. no. 381. [Online]. Available: https://www.mdpi.com/2304-6732/9/6/381

[43] Y. Kim et al., "Semi-random multicore fibre design for adaptive multiphoton endoscopy," *Opt. Exp.*, vol. 26, no. 3, Feb. 2018, Art. no. 3661. [Online]. Available: https://opg.optica.org/abstract.cfm?URI=oe-26-3-3661

[44] C. Xia, N. Bai, I. Ozdur, X. Zhou, and G. Li, "Supermodes for optical transmission," *Opt. Exp.*, vol. 19, no. 17, pp. 16653–16664, 2011.

[45] C. Xia et al., "Supermodes in coupled multi-core waveguide structures," *IEEE J. Sel. Topics Quantum Electron.*, vol. 22, no. 2, pp. 196–207, Mar./Apr. 2016. [Online]. Available: https://ieeexplore.ieee.org/document/7279062/

[46] M. Koshiba, K. Saitoh, K. Takenaga, and S. Matsuo, "Multi-core fiber design and analysis: Coupled-mode theory and coupled-power theory," *Opt. Exp.*, vol. 19, no. 26, pp. B102–B111, Dec. 2011. [Online]. Available: https://opg.optica.org/oe/abstract.cfm?uri=oe-19-26-B102

[47] W. Ren, Z. Tan, and G. Ren, "Analytical formulation of supermodes in multicore fibers with hexagonally distributed cores," *IEEE Photon. J.*, vol. 7, no. 1, Feb. 2015, Art. no. 7100311. [Online]. Available: https://ieeexplore.ieee.org/document/7018018/

[48] W. Jin and S. Jian, "Numerical and simulation analyses on supermode characteristics of dual-core fiber and four-core fiber," *Optik*, vol. 132, pp. 32–38, Mar. 2017. [Online]. Available: https://linkinghub.elsevier.com/retrieve/pii/S0030402616315923

[49] Y. Huo, P. K. Cheo, and G. G. King, "Fundamental mode operation of a 19-core phase-locked Yb-doped fiber amplifier," *Opt. Exp.*, vol. 12, no. 25, Dec. 2004, Art. no. 6230. [Online]. Available: https://opg.optica.org/abstract.cfm?URI=oe-12-25-6230

[50] Y. Sasaki, K. Takenaga, K. Aikawa, Y. Miyamoto, and T. Morioka, "Single-mode 37-Core fiber with a cladding diameter of 248 μm," in *Proc. Opt. Fiber Commun. Conf.*, 2017, Ppaer Th1H.2. [Online]. Available: https://opg.optica.org/abstract.cfm?URI=OFC-2017-Th1H.2

[51] L. Wu et al., "Deep learning: High-quality imaging through multi-core fiber," *Curr. Opt. Photon.*, vol. 4, no. 4, pp. 286–292, Aug. 2020, doi: 10.3807/COPP.2020.4.4.286.

[52] K. L. Reichenbach and C. Xu, "Independent core propagation in two-core photonic crystal fibers resulting from structural nonuniformities," *Opt. Exp.*, vol. 13, no. 25, 2005, Art. no. 10336. [Online]. Available: https://opg.optica.org/oe/abstract.cfm?uri=oe-13-25-10336

[53] G. T. Jasion et al., "Fabrication of tubular anti-resonant hollow core fibers: Modelling, draw dynamics and process optimization," *Opt. Exp.*, vol. 27, no. 15, Jul. 2019, Art. no. 20567. [Online]. Available: https://opg.optica.org/abstract.cfm?URI=oe-27-15-20567

[54] G. P. Agrawal, *Applications of Nonlinear Fiber Optics*, 3rd ed. London, U.K.: Academic Press, 2021.

[55] B. J. Ávila, J. N. Hernández, S. M. T. Rodríguez, and B. M. Rodríguez-Lara, "Symmetric supermodes in cyclic multicore fibers," *OSA Continuum*, vol. 2, no. 3, Mar. 2019, Art. no. 515. [Online]. Available: https://opg.optica.org/abstract.cfm?URI=osac-2-3-515

[56] G. Peng, T. Tjugiarto, and P. Chu, "Polarisation beam splitting using twin-elliptic-core optical fibres," *Electron. Lett.*, vol. 26, no. 10, pp. 682–683, May 1990. [Online]. Available: https://digital-library.theiet.org/content/journals/10.1049/el_19900446

[57] F. Y. M. Chan, A. P. T. Lau, and H.-Y. Tam, "Mode coupling dynamics and communication strategies for multi-core fiber systems," *Opt. Exp.*, vol. 20, no. 4, Feb. 2012, Art. no. 4548. [Online]. Available: https://opg.optica.org/oe/abstract.cfm?uri=oe-20-4-4548

[58] N. Mothe and P. D. Bin, "Numerical analysis of directional coupling in dual-core microstructured optical fibers," *Opt. Exp.*, vol. 17, no. 18, pp. 15778–15789, 2009.

[59] K. L. Reichenbach and C. Xu, "The effects of randomly occurring nonuniformities on propagation in photonic crystal fibers," *Opt. Exp.*, vol. 13, no. 8, 2005, Art. no. 2799. [Online]. Available: https://opg.optica.org/oe/abstract.cfm?uri=oe-13-8-2799

[60] L. Li et al., "Phase locking and in-phase supermode selection in monolithic multicore fiber lasers," *Opt. Lett.*, vol. 31, no. 17, pp. 2577–2579, 2006.

Md Abu Sufian received the B.S. degree in electrical and electronic engineering from the Khulna University of Engineering and Technology, Khulna, Bangladesh, in 2015, and the M.S. degree in materials and devices from Electrical and Computer Engineering Department, University of Delaware, Newark, DE, USA, in 2020. Since 2020, he has been working toward the Ph.D. degree with the Center for Research and Education in Optics and Lasers, College of Optics and Photonics, University of Central Florida, Orlando, FL, USA. His research interests include design, fabrication, and characterization of new generation hollow core fibers, fiber bundles and components for imaging applications, laser systems, and fiber optic communications.

Erwan Baleine received the Ph.D. degree in optical science from the College of Optics and Photonics, University of Central Florida, Orlando, FL, USA. In 2017, he joined the Applied Research Group, Lockheed Martin, where he is currently an Associate Fellow. His research interests include optical waveguides and microstructures for optical applications.

Jeffrey Geldmeier received the B.S. degree in materials science from Virginia Tech, Blacksburg, VA, USA, in 2012, and the Ph.D. degree in materials science from Georgia Tech, Atlanta, GA, USA, in 2017. In 2021, he joined Lockheed Martin, Bethesda,, MD, USA, as an Optical Engineer where his current interests include nanostructured surfaces and IR material characterization.

Ameen Alhalemi received the B.Sc. degree in physics from Taiz University, Taiz, Yemen, in 2009, and the M.Sc degree in photonics from The City University of New York, Queens College, Queens, NY, USA in 2020. Since 2022, he has been working toward the Ph.D. degree with the Center for Research and Education in Optics and Lasers, College of Optics and Photonics, University of Central Florida, Orlando, FL, USA. His research interests include optical fiber and materials, hollow core fiber, and laser systems.

Jose Enrique Antonio-Lopez received the Ph.D. degree from the Instituto Nacional de Astrofísica, Óptica y Electrónica (INAOE), Puebla, Mexico, in 2012, with the work design and fabrication of photonic devices based on multimode interference. He is currently a Research Scientist with the College of Optics and Photonics (CREOL), University of Central Florida, Orlando, FL, USA. His research interests include design, fabrication, and use of special fibers.

Rodrigo Amezcua-Correa (Member, IEEE) received the Ph.D. degree from Optoelectronics Research Centre, University of Southampton, Southampton, U.K. in 2009. Since 2011, he has been with the College of Optics and Photonics, University of Central Florida, Orlando, FL, USA, where he is currently a Professor of optics and photonics. His research interests include fiber design and fabrication for applications including communications, fiber lasers, nonlinear optics, and sensing.

Axel Schülzgen (Fellow, IEEE) received the Ph.D. degree in physics from the Humboldt University of Berlin, Berlin, Germany. Since 2009, he has been a Professor of optics and photonics with the Center for Research and Education in Optics and Lasers, College of Optics and Photonics, University of Central Florida, Orlando, FL, USA. He is currently an Adjunct Professor with the College of Optical Sciences, University of Arizona, Tucson, AZ, USA. His current research interests include optical fiber devices, components, materials, and structures with applications in fiber laser systems, fiber optic sensing and imaging, and optical communications. Dr. Schülzgen is a Fellow of the Optica and the International Society for Optics and Photonics SPIE.